FISEVIER

Contents lists available at ScienceDirect

Journal of the European Ceramic Society

journal homepage: www.elsevier.com/locate/jeurceramsoc





A novel room-temperature synthesis technique for producing high-density $Ba_{1-x}Sr_xTiO_3$ and $PbZr_yTi_{1-y}O_3$ composites

Evan Smith a,*, Alison Block b, Rick Ubic a

- ^a Micron School of Materials Science & Engineering, Boise State University, 1910 University Drive, Boise, ID 83725, USA
- ^b Department of Chemistry, Carleton College, 1 North College Street, Northfield, MN 55057, USA

ABSTRACT

The ability to synthesize capacitors at room temperature has great cost-saving potential compared to energy-intensive conventional sintering techniques which involve extended periods at high temperature. In this work, several compositions in the $Ba_{1-x}Sr_xTiO_3$ (BST) and $PbZr_yTi_{1-y}O_3$ (PZT) series were synthesized conventionally and densified via a room-temperature fabrication (RTF) process. The BST and PZT particles were coated and mixed with an aqueous solution of Li_2MoO_4 (LMO), which acts as a binder. The novel techniques presented in this work, including the usage of a vacuum-assisted pellet die and a bath sonicator in combination, were designed to increase the density of the resultant pellets. Relative densities as high as 96.1% were achieved for BST x=0.5, 96.9% for BST x=0.45%, and 95.1% for PZT y=0.5 RTF pellets using LMO as a binder. These composites are the densest room-temperature fabricated composites reported to date. In addition, the effect of mixing particles with two different size distributions was analyzed for composites produced with PZT particles. The dielectric properties of all these dense RTF composites were measured at temperatures ranging from 150 °C to -60 °C and compared with those of conventionally sintered electroceramics with the same compositions.

1. Introduction

This work aims to improve upon the novel room-temperature fabrication (RTF) technique recently developed[1-3] for synthesizing electroceramics at room temperature. The approach involves coating microparticles of electoceramic material with functional inorganic binders using a solution-based processing technique. Slurries are uniaxially pressed in a pellet die and dried at room temperature or in a drying oven. A similar approach has been used to densify bulk structural ceramics[4]. The only binder phase investigated to date is Li₂MoO₄ (LMO).[1,2] While V₂O₅[5], Na₂Mo₂O₇,[5] and K₂Mo₂O₇[5] have been found to effectively densify when used in the cold-sintering process, they have yet to be used in this RTF technique. A major advantage of RTF is that it can produce composites that contain as much as 75% of the electroceramic material, which is important in order to preserve useful dielectric properties; however, the densest composites so far reported[1, 2] still contain about 10% porosity. Clearly, there remains some significant work to be done in order to reduce the amount of porosity within these composites, which will inherently result in an improvement in dielectric properties.

The RTF technique has recently been applied to produce Ba_1 . $_xSr_xTiO_3$ (BST),[1] Pb $Zr_yTi_{1-y}O_3$ (PZT),[2] and $SrTiO_3$ [3] composites using Li_2MoO_4 as a binder material. One critical processing parameter is

the starting particle size of the electroceramic material. Kuzmic[3] has investigated five size ranges and mixtures of different size ranges using $SrTiO_3$: $< 40 \mu m$, $150-200 \mu m$, $200-500 \mu m$, 75% $150-200 \mu m + 25\%$ <40 μm , and 75% 200–500 $\mu m + 14\%$ 63–40 $\mu m + 11\% <$ 40 μm . When pressed for 5 min at 250 MPa the composites achieved relative densities of ~76%, 81%, 84%, 83%, and 84%; and permittivities of 46, 65, 70, 67, and 73, respectively. Another parameter that they investigated was the amount of time that the composites were pressed at a particular pressure. They found no difference in the final density when the composites were pressed at 250 MPa for 1, 5, 10, 20, or 60 min[3]. Thus, the density appears to be independent of time under pressure. Additionally, the effect of pressure itself was analyzed. Composites were pressed for 5 min at 60, 130, 250, 500, and 1000 MPa. It was noted[3] that the densities gradually increased from about 82-87% as the pressure was increased to 1000 MPa. Interestingly, the permittivity decreased and the dielectric loss increased with increasing pressure, which they attributed to the fracturing of large electroceramic grains at higher pressures.

The effect of sonication on densification has also been investigated by Kuzmic et al.,[3] who immersed the powder-containing pellet die in a bath sonicator for a period of time before removing it for pressing. The duration of immersion varied between 0, 0.5, 1, 2, and 5 min. While the density did not improve as a result of this procedure, the permittivity and dielectric losses were both observed to increase with increasing

E-mail address: EvanSmith246@BoiseState.edu (E. Smith).

 $^{^{\}ast}$ Corresponding author.

immersion time. Interestingly, the effects of drying time were also examined[3] and it was observed that when the composites were dried quickly in a drying oven the permittivity was negatively affected even though there was absolutely no effect on the density.

Nelo et al.[1] investigated the effect of the particle size on the dielectric properties of BST. It was found that particles in the size range $180\text{--}425\,\mu\text{m}$ produced composites with larger relative permittivities and lower loss tangents than composites made with particles in the size range $63\text{--}180\,\mu\text{m}$. Overall, composites with the larger particles exhibited $\epsilon_r\sim425$ and $\tan\delta\sim0.325$ at 20 Hz, and $\epsilon_r\sim200$ and $\tan\delta\sim0.02$ at 1 MHz; whereas composites with smaller particles had $\epsilon_r\sim360$ and $\tan\delta\sim0.41$ at 20 Hz, and $\epsilon_r\sim150$ and $\tan\delta\sim0.02$ at 1 MHz. For the PZT composites, Nelo et al.[2] used bimodal mixtures of particle sizes including 90 wt% of particles in the size range $180\text{--}425\,\mu\text{m}$ and 10 wt% of particles with an average size of $6\,\mu\text{m}$. Composites made with this mixture exhibited $\epsilon_r\sim244$ and $\tan\delta\sim0.09$ at 20 Hz, and $\epsilon_r\sim200$ and $\tan\delta\sim0.013$ at 1 MHz.

While the cold sintering process (CSP) is fundamentally different from RTF, there are several similarities between the two techniques and useful information can be gleaned by studying CSP composites. Several low-permittivity materials, including Li₂MoO₄, Na₂Mo₂O₇, (LiBi)_{0.5} MoO₄, and K₂Mo₂O₇ were successfully densified[1,2,5,6] by the CSP process. Guo et al. have successfully fabricated Li₂MoO₄, Na₂Mo₂O₇, K₂Mo₂O₇, and V₂O₅ ceramics to densities of 95.7%, 93.7%, 94.1%, and 90.2%, respectively; all at 120 °C and a pressure of 350 MPa.[5] They even cold-sintered NaCl to a density of 90.0% by pressing NaCl powder at 5 MPa then exposing it to humidity at room temperature for up to 24 hrs. [5] It is also possible to produce refractory ceramics via the CSP. Guo et al. used the CSP at 180 °C to manufacture yttria-doped zirconia-based ceramics that had a Vickers hardness of 0.5 GPa and densities as high as 85%.[7] Although such ceramics aren't nearly as hard as conventionally sintered yttria-doped zirconia (10-13 GPa), subsequent annealing of this CSP pellet at 1000 °C improved its hardness to 10.5 GPa.

Additionally, Funahashi et al. have successfully produced ZnO compacts with densities > 90% using the CSP.[8] ZnO compacts were cold-sintered at 120 $^{\circ}\text{C}$ and 305 $^{\circ}\text{C},$ and the conductivities of these samples were observed to be 0.00002 and 9 S/cm, respectively. The latter value is comparable to the conductivity of ZnO conventionally sintered at 1400 °C. Both Guo et al.[9] and Tsuji et al.[10] have had success with cold-sintering BaTiO3 ceramics for ferroelectric applications. BaTiO₃ compacts produced with nanopowders with an average particle size of 75 nm and 150 nm were successfully densified to 92% and 96% of theoretical density, respectively. These compacts were held at 520 MPa and 300 °C for 12 hrs.[10] Remarkably, at 1 MHz these dense compacts showed[10] $\varepsilon_r = 690$ and 1830 at room temperature, respectively, with $tan\delta \sim 0.04$, comparable to BaTiO₃ ceramics produced via conventional high-temperature sintering techniques. More recently, PbZr_vTi_{1-v}O₃ piezoelectrics with $\epsilon_r = 207$ at 100 kHz and $d_{33} =$ 4 pC/N were synthesized to 89% of theoretical density under a pressure of 500 MPa at 300 °C.[11] Subsequent annealing of these pellets at 700 °C and 900 °C produced compacts that were 91% and 99% of theoretical density with $\epsilon_r=$ 917, $d_{33}=$ 80 pC/N and $\epsilon_r=$ 1324, $d_{33}=$ 197 pC/N, respectively.

In this work, perovskite phases in the series $Ba_{1-x}Sr_xTiO_3$ and $PbZr_yTi_{1-y}O_3$ were synthesized from oxide powders via conventional solid-state processing techniques for use in the RTF process, and Li_2MoO_4 was used as the binding material for all composites. The goal of this work was to improve the density of these composites by reducing the porosity through several novel methods. In particular, the particles were pressed inside a vacuum-assisted pellet die under high vacuum for a period of time. The pellet die was then removed from the press and immersed in a bath sonicator for a period of time. This process was repeated up to ten times to achieve relative densities as high as 96.1%. Ultimately, this process results in composites with higher percentages of electroceramic material as compared to the composites produced previously; hence, this process leads to composites with higher

permittivities than previously reported via the RTF method.

2. Materials & methods

2.1. Conventional pellet preparation and particle size classification

Compounds in the Ba_{1-x}Sr_xTiO₃ system were synthesized via the solid-state mixed-oxide route. Stoichiometric amounts of BaCO₃ (99.8%, Alfa-Aesar, Thermo Fisher Scientific, Tewksbury, MA), SrCO₃ (>99%, Alfa-Aesar, Ward Hill, MA), and TiO2 (99.5%, Alfa-Aesar, Ward Hill, MA) were ball-milled with yttria-stabilized ZrO2 (YSZ) media using deionized water in a high-density nylon pot for about six hours. Powders were then dried overnight in an atmospheric drying oven at \sim 98 $^{\circ}$ C until all the water was evaporated. Calcination was conducted for five hours in a muffle furnace (1807FL, CM Furnaces Inc., Bloomfield, NJ) at 1150 °C. After calcination, the powders were ball-milled again for \sim 24 h with YSZ media using deionized water in a high-density nylon pot, adding 2 wt% polyethylene glycol (PEG 10,000, Alfa-Aesar, Heysham, UK) powder for the final five minutes. The mixtures were then dried overnight in an atmospheric drying oven at ~98 °C until all the water was evaporated. Cylindrical green compacts 8-10 mm in height and 20 mm in diameter were then formed by applying a uniaxial pressure of 63 MPa. Compacts were then sintered on an alumina plate for 4 h at 1350 °C. After sintering, the dense pellets were then pulverized using a percussion mortar and pestle. The resultant powder was then classified into two size ranges: $\emptyset < 180 \ \mu m$ and $180 \ \mu m \le \emptyset \le 500 \ \mu m$.

Additionally, in an effort to increase the particle size whilst simultaneously reducing the amount of energy spent on sintering, some as-mixed powder was calcined for 12 h at 1500 $^{\circ}\text{C}.$ The resulting particles were then sieved to under 500 $\mu m.$

Compositions in the system PbZr_yTi_{1-y}O₃ were also synthesized via the solid-state mixed oxide route. Stoichiometric amounts of PbO (99.9%, Alfa-Aesar, Ward Hill, MA), ZrO₂ (>99%, Alfa-Aesar, Ward Hill, MA), TiO2 (99.5%, Alfa-Aesar, Ward Hill, MA) were ball-milled with yttria-stabilized ZrO2 (YSZ) media using deionized water in a highdensity nylon pot for about six hours. Powders were then dried overnight in an atmospheric drying oven at ~98 °C until all the water was evaporated. Calcination was conducted in a pre-contaminated closed crucible for two hours in a muffle furnace (1807FL, CM Furnaces Inc., Bloomfield, NJ) at 850 °C. After calcination, the powders were ballmilled again for ~24 h with YSZ media using deionized water in a high-density nylon pot. The calcined powder was then dried overnight in an atmospheric drying oven at ~98 °C until all the water was evaporated. Cylindrical green compacts 8-10 mm in height and 20 mm in diameter were then formed by applying a uniaxial pressure of 63 MPa. Compacts were placed on a bed of sacrificial calcined powder of the same composition on an inverted Al₂O₃ crucible lid and were completely covered with the same sacrificial powder to induce a lead-rich closed atmosphere during sintering. An inverted 250 ml Al₂O₃ crucible was placed over the inverted Al₂O₃ lid containing the compacts and sacrificial powder. Compacts were sintered for two hours at 1150 °C. After sintering, the dense pellets were then crushed using a percussion mortar and pestle and the resulting powder was classified into two size ranges: ϕ < 180 μm and 180 $\mu m \leq \emptyset \leq$ 500 $\mu m.$

2.2. RTF pellet preparation

The BST and PZT particles produced were coated with a thin layer of Li_2MoO_4 (>99%, Alfa-Aesar, Ward Hill, MA) by first dissolving 10 vol% Li_2MoO_4 in 2 ml of deionized water in the case of BST and 10–19 vol% Li_2MoO_4 in the case of PZT. Then 20 ml of 1,2-butanediol (>98%, TCI America, Portland, OR) was mixed into the solution. The $\text{Ba}_{1-x}\text{Sr}_x\text{TiO}_3$ or PbZryTi_{1-y}O₃ particles were then added to the mixture. In the case of PZT, Li_2MoO_4 was also dissolved in 10 ml of deionized water before adding 10 ml of 1,2-butanediol for several particle mixtures. The mixture was heated to 150 °C to drive off all the water and most of the

1,2-butanediol. When the mixture turned into a thick paste, it was spread evenly on a petri dish and placed in a drying oven at 150 $^{\circ}$ C for about 12 h to drive off the rest of the 1,2-butanediol.

Then 1 g of the coated particles was mixed with 0.25 ml of a saturated solution of $\rm Li_2MoO_4$ in deionized water. The slurry is then placed in a 13 mm pellet die and pressed to a target pressure using a uniaxial pellet press (Atlas 15-ton press, Specac Ltd., Orpington, UK). Pressure was maintained for five minutes, after which the die was placed into a bath sonicator (Branson Model 2800-DTH, Branson Ultrasonics, Brookfield, CT). The sonicator was run at full power for one minute, after which the die was returned to the press and uniaxially pressed to the target pressure again for five minutes. This sonication step was repeated up to ten times. This same procedure was also performed using a 13 mm evacuable pellet die (Specac Ltd., Orpington, UK) connected to a rotary vane vacuum pump (Robinair 15500, Bosch Automotive Solutions Inc., Warren, MI) to aid liquid removal and so facilitate densification. This procedure is outlined in Fig. 1.

The density of RTF pellets was measured via a combination of a micrometer screw gauge (Insize Co., Loganville, GA) with an accuracy of $\pm~0.002$ mm and the buoyancy (Archimedes') method in ethanol using a density measuring kit (Mettler Toledo, Columbus, OH). The density of conventionally sintered pellets was measured only with the buoyancy method in deionized water.

2.3. XRD, TEM, and dielectric measurements

Powder XRD measurements were performed in a diffractometer (Miniflex-600, Rigaku, Woodlands, TX) operating with convergent-beam geometry and CuK α radiation. Le Bail refinements were performed using GSAS II.[12] The background was fitted with a sixth-order Chebychev polynomial. All Ba_{1-x}Sr_xTiO₃ compositions (x=0.3, 0.45, and 0.5) were fitted with cubic symmetry. The PbZr_yTi_{1-y}O₃ y=0.5 and 0.52 compositions were fitted assuming that both tetragonal (P4mm) and trigonal ($R\overline{3}c$) PZT phases co-exist, whereas the y=0.6 composition was fitted with trigonal symmetry only.

RTF specimens for scanning electron microscopy were mounted in epoxy and ground/polished using conventional ceramographic techniques (Labopol 5, Struers, Cleveland, OH), finishing with a 1 μ m diamond paste. The microstructures were analyzed via a field emission scanning electron microscope (Teneo, FEI, Hillsboro, OR). Energy

dispersive spectroscopy (EDS) measurements were performed on the microstructures using the AZtecEnergy Advanced Microanalysis System with X-MaxN 80 large area analytical silicon-drift detector (Oxford Instruments, Concord, MA). Specimens for transmission electron microscopy (TEM) (JEM-2100 HR, JEOL, Japan) were prepared by dusting some fine powder onto a holey carbon TEM grid.

Electrical measurements were recorded using an LCR meter (model E4980A, Keysight Technologies, Santa Rosa, CA) setup for parallel-plate capacitors. The faces of each RTF and conventionally sintered pellet were metalized with a thin layer of conductive paint (Electrodag 1415 M, Electron Microscopy Sciences, Hatfield, PA) before testing. The pellets were then inserted into an in-house high-temperature-tolerant dielectric-testing fixture which consists of two gold-plated, spring-loaded needles cemented into place by a PTFE fixture. This fixture is encapsulated inside an aluminum box with a removable lid. High-temperature-tolerant coaxial cables are attached to the ends of the needles which allow for data transmission to the LCR meter. This fixture was placed inside a temperature chamber (ESPEC SU-262, ESPEC Corp., Osaka, Japan). Dielectric measurements were recorded at a frequency of 1 kHz upon cooling from 150 °C to -60 °C at a ramp rate of -1 °C/min.

3. Results & discussion

As-calcined $Ba_{1-x}Sr_xTiO_3$ (x=0.3, 0.45, and 0.5) powders were analyzed via X-ray diffraction to verify phase purity, as can be seen in Fig. 2. The tetragonal-to-cubic phase boundary for BST generally occurs around the x=0.3 composition at room temperature; hence, all compositions produced in this work should exhibit cubic symmetry. Indeed the x=0.3, 0.45, and 0.5 compositions were well fitted with cubic symmetry using Le Bail refinements as shown in Table 1, which agrees with previous reports for similar compositions[13].

Additionally, as-calcined $PbZr_yTi_{1,y}O_3$ (y=0.5, 0.52, and 0.6) powders were analyzed for phase purity via X-ray diffraction (Fig. 3). The y=0.6 composition clearly consists of a single PZT phase with trigonal symmetry; however, both the y=0.5 and 0.52 compositions contain both tetragonal and trigonal phases. It is well documented [14, 15] that PZT exhibits a morphotropic phase boundary (MPB) at $y\sim0.52$, exhibiting tetragonal symmetry for compositions with y<0.52 and trigonal symmetry for compositions with y>0.52; thus, it is a

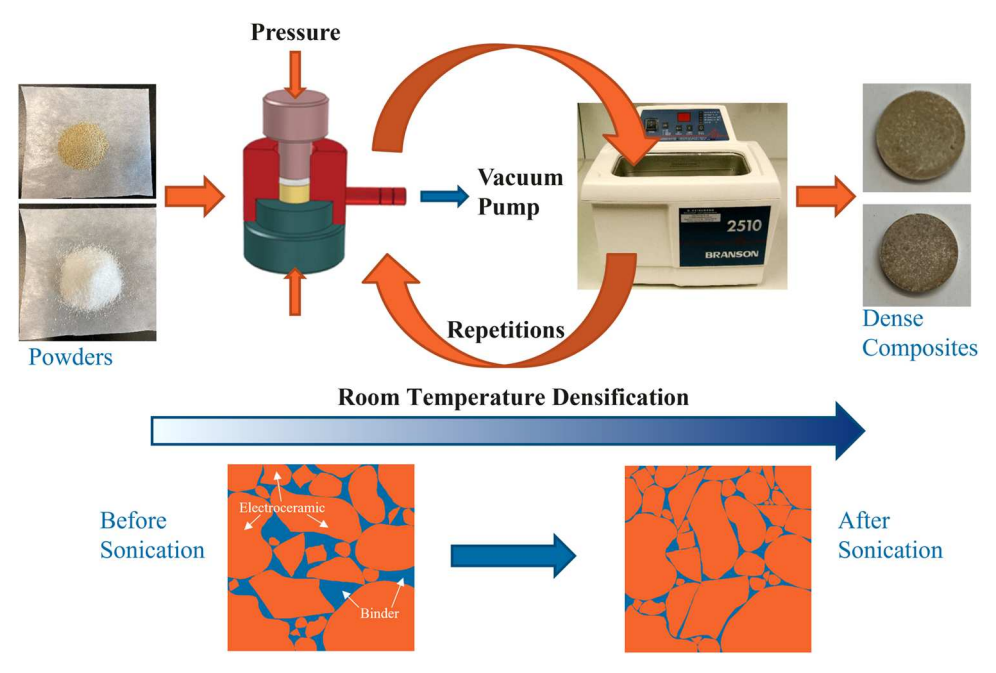


Fig. 1. Schematic showing the room-temperature densification process.

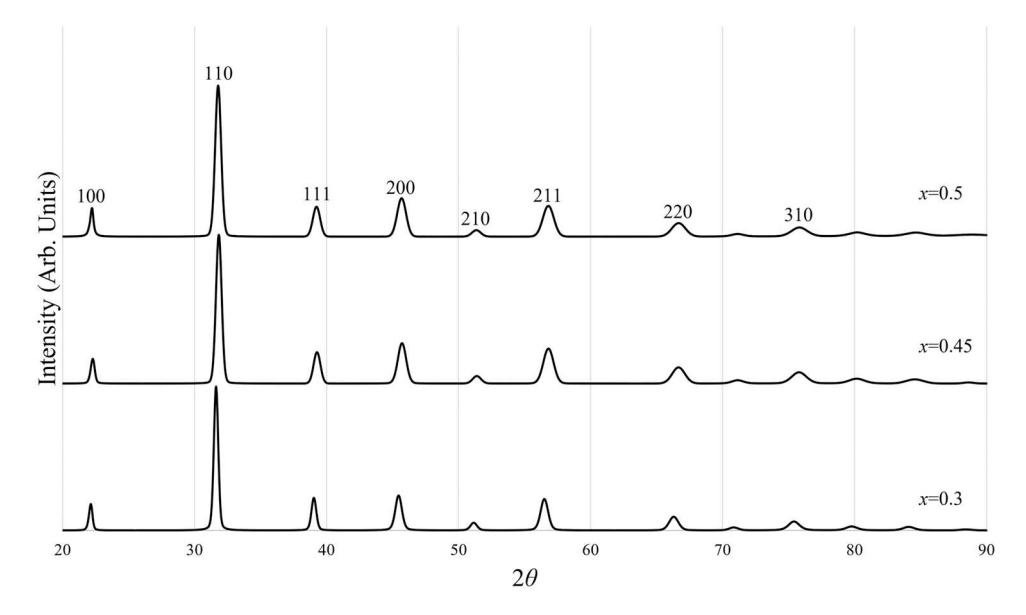


Fig. 2. XRD patterns of BST x = 0.3, 0.45, and 0.5 compositions indexed according to cubic unit cells in $Pm\overline{3}m$.

Table 1Refined cubic lattice constants for Ba_{1-x}Sr_xTiO₃ powders.

Composition	a (Å)
x = 0.3 $x = 0.45$ $x = 0.5$	3.9827(2) 3.9720(4) 3.9667(3)

reasonable assumption that compositions near the MPB ($y=0.5~{\rm or}~0.52$) would contain both tetragonal and trigonal phases. The $y=0.5~{\rm and}~0.52$ patterns in Fig. 2 are only indexed with tetragonal indices for the sake of convenience; although, the trigonal peaks can also be clearly seen in those patterns. No other phases were observed. Table 2 shows the refined tetragonal and trigonal lattice constants for these PZT compounds.

Fig. 4 shows a cluster of several sub-micron sized BaTiO₃ particles coated with LiMoO₄. This evidence clearly demonstrates that the coating

procedure is effective and in adequately coating the electroceramic particles. Although several small $BaTiO_3$ particles are encapsulated together with the $LiMoO_4$, the cluster is only about $1~\mu m$ in size, implying that smaller ($<0.5~\mu m$) particles may become encapsulated by the binder material and become deposited along with the binder material around larger particles. Unfortunately, it was not possible to analyze larger particles using this technique due to the fact the TEM requires electron transparency. It should also be noted that $BaTiO_3$ particles were used here because $BaTiO_3$ is the x=0 end member of the BST system and of all the compositions studied it had the smallest particle size. Fig. 4 will look very similar for LMO-coated BST (x \ddagger 0) and PZT particles because only very small particles are visible in the TEM.

Table 3 shows the various techniques used to improve the density of these RTF composites. Initially, composites were routinely produced with densities around 85.5%, as determined via the dimensions and mass of the pellets. One of the most effective techniques that was used to improve densification was immersing the pellet die into a bath sonicator after the initial pressing and then re-pressing. Table 3 shows the

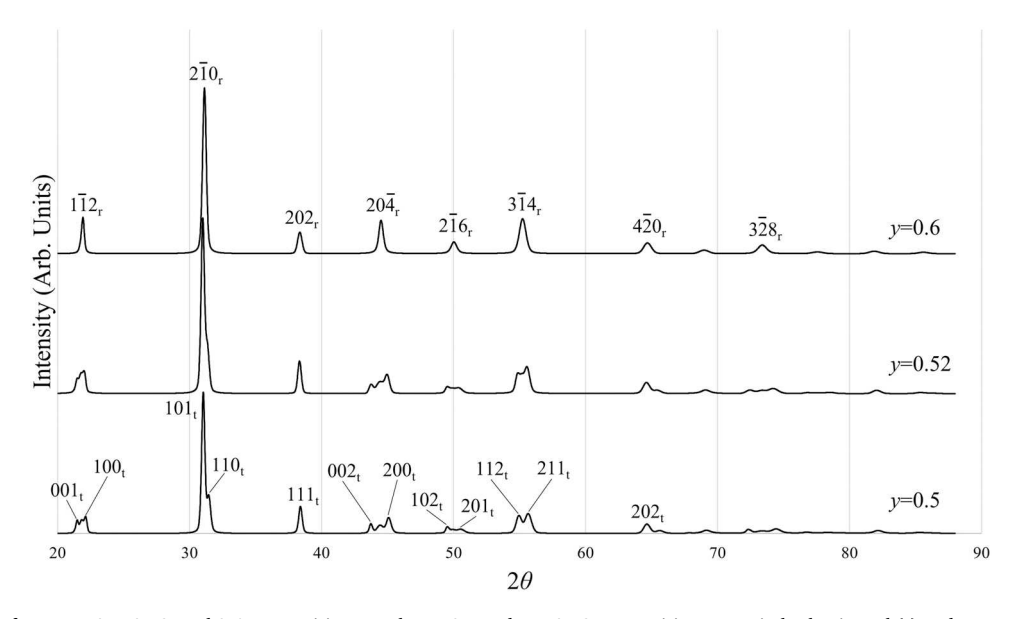


Fig. 3. XRD patterns of PZT y = 0.5, 0.52, and 0.6 compositions. Both y = 0.5 and y = 0.52 compositions contain both trigonal (r) and tetragonal (t) peaks, but only the latter are indexed here due to limited space. The y = 0.6 composition contains only the trigonal phase.

Table 2 Refined lattice constants for $PbZr_{\nu}Ti_{1-\nu}O_3$ powders.

Composition	a_t (Å)	c_t (Å)	a_r (Å)	c_r (Å)	α (°)	γ(°)
y = 0.5	4.0237 (1)	4.1392 (2)	5.7626(7)	14.207(15)	90	120
y = 0.52	4.0300 (1)	4.1316 (2)	5.7570(6)	14.200(14)	90	120
y = 0.6	-	-	5.7616(4)	14.2127(6)	90	120

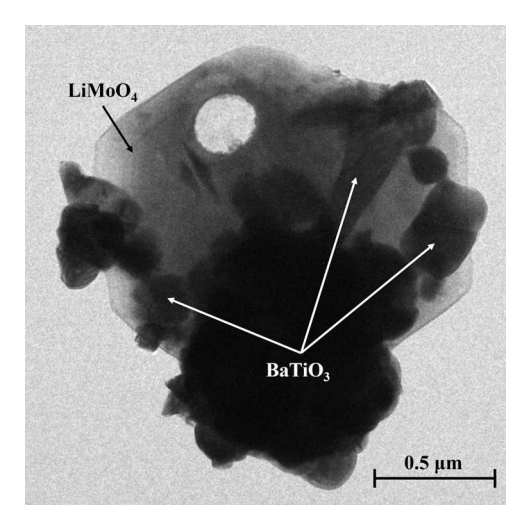


Fig. 4. TEM image of a cluster of BaTiO₃ particles coated with LiMoO₄.

effectiveness of increasing the number of iterations of this process. The density gradually increased to around 89.5% as the number of sonication treatments was increased to five.

Interestingly, increasing the immersion time in the sonicator to 5 min and increasing the time under pressure to 10 min had no effect on the density of composites. Thus, for the sake of efficiency, the immersion

time was limited to 1 min and the pressing time was limited to 5 min per iteration.

Using a vacuum-assisted pellet die with a 60 Torr vacuum applied to the system also had a significant effect on the density. In fact, after performing five iterations under vacuum, the density of these BST-LMO composites was improved to about 90.9%. The density was further improved to about 92.1% by increasing the number of repetitions to 10 under the same conditions.

Another factor that improved the density of these pellets was an increase in pressure. Specifically, the pressure was incrementally increased up to 700 MPa. Remarkably, the density improved up to about 94.5% at a pressure of 650 MPa using 5 iterations. Increasing the pressure even further resulted in no improvement. Further increasing the number of repetitions to 10 resulted in pellets that were about 96.1% dense as measured via the buoyancy method in ethanol.

Since increasing the pressure to 650 MPa under vacuum resulted in a 4-5% improvement in density, the effects of pressure were then investigated without using a vacuum. A series of RTF composites were produced with a pressing pressure of 650 MPa with 0 - 5 sonication iterations. The density slightly improved from about 90.5% up to 91.9% at four iterations, after which no noticeable improvement was observed. This evidence demonstrates that increasing the pressure from 250 MPa to 650 MPa alone results in an approximately 5% increase in the density of BST composites, even without sonication; however, the sonication procedure clearly plays an important role in the densification process because the composite pressed at 650 MPa with five sonication iterations had a density about 1.5% higher than that of the composite pressed at 650 MPa without sonication. It is also evident that the vacuum plays an important role in densification as the composites pressed at 650 MPa under vacuum are about 3% denser than the composites pressed at 650 MPa with no vacuum.

The relative densities of BST pellets made directly from powders calcined at 1500 °C using 10 vol% LMO as a binder range from 95.5% to 96.9%. These results are important because they show that smaller particles (< 180 μm) can be incorporated into RTF pellets whilst maintaining a high degree of densification.

Energy dispersive X-ray spectroscopy mapping was performed on a

Table 3 Density improvement of $Ba_{1.x}Sr_xTiO_3 - Li_2MoO_4$ composite RTF pellets using different techniques. All pellets contain 10 vol% LMO. All densities were measured using the buoyancy method in ethanol unless otherwise noted.

BST Compound	Particle sizes (µm)	Time under pressure (min.)	Pressure (MPa)	Sonication time (min.)	Repetitions	Vacuum (Torr)	Density (%)
x = 0.5	180-500	5	250	0	0	760	85.5 *
x = 0.5	180-500	5	250	1	1	760	85.9 *
x = 0.5	180-500	5	250	1	2	760	86.7 *
x = 0.5	180-500	5	250	1	3	760	87.3 *
x = 0.5	180-500	5	250	1	4	760	88.9 *
x = 0.5	180-500	5	250	1	5	760	89.5
x = 0.5	180-500	5	250	1	5	60	90.9
x = 0.5	180-500	5	250	5	5	60	90.5
x = 0.5	180-500	10	250	1	5	60	90.4
x = 0.5	180-500	5	250	1	10	60	92.1
x = 0.5	180-500	5	350	1	5	60	91.2
x = 0.5	180-500	5	450	1	5	60	92.1
x = 0.5	180-500	5	550	1	5	60	93.3
x = 0.5	180-500	5	650	1	5	60	94.5
x = 0.5	180-500	5	700	1	5	60	94.4
x = 0.5	180-500	5	650	1	10	60	96.1
x = 0.5	180-500	5	700	1	10	60	96.1
x = 0.5	180-500	5	650	0	0	760	90.5
x = 0.5	180-500	5	650	1	1	760	90.7
x = 0.5	180-500	5	650	1	2	760	91.4
x = 0.5	180-500	5	650	1	3	760	91.7
x = 0.5	180-500	5	650	1	4	760	91.9
x = 0.5	180-500	5	650	1	5	760	91.8
x = 0.5	1-500	5	650	1	10	60	95.5 *
x = 0.45	1-500	5	650	1	10	60	96.9
x = 0.3	1–500	5	650	1	10	60	95.8

^{*}Density measured via the outer dimensions and mass of the pellets.

cross-section of a $Ba_{0.5}Sr_{0.5}TiO_3 - Li_2MoO_4$ composite pellet that was 95.5% dense as measured via its outer dimensions and mass. The results of the mapping (Fig. 5) show that Li_2MoO_4 is relatively evenly distributed between the $Ba_{0.5}Sr_{0.5}TiO_3$ particles as designed. This result is important because it also shows that Li_2MoO_4 does not clump as the pellets dry. This SEM image also highlights the low porosity within the pellet, which is shown by the colorless regions in the image.

Fig. 6 shows the permittivities and dielectric losses of two BST-LMO composite RTF pellets produced using BST x = 0.45 and x = 0.3 particles from powder that was calcined at 1500 °C for 12 h and then sieved to under 500 μm . The resultant pellets were measured to be 96.9% and 95.3% dense, respectively, according to the buoyancy method in ethanol. Additionally, Fig. 7 shows the permittivities and dielectric losses of two pure BST pellets with x = 0.45 and x = 0.3 compositions. The densities of these two pellets were measured via the buoyancy method in deionized water as 98.0% and 97.0% of theoretical density, respectively. As expected, the permittivities are lower for BST-LMO composites than for conventionally sintered pure BST, with maximum values an order of magnitude lower than the conventionally produced pellets. The sharpness (temperature sensitivity) of the curves near T_C is also greatly reduced. Interestingly, the dielectric losses of the RTF pellets gradually decrease with decreasing temperature from 150 $^{\circ}$ C to -60 $^{\circ}$ C instead of peaking near T_C, as is the case for conventionally sintered pellets. The dielectric losses of RTF BST are also relatively high at high temperatures; however, their room-temperature losses are comparable to those measured from conventionally sintered pellets.

Table 4 shows the Curie temperatures for both the RTF composites and the conventionally sintered BST pellets. Interestingly, T_C was measured to be about 11–15 °C lower for the conventional pellets than for the RTF pellets. This discrepancy could potentially be due to the slight solubility of the binder material in BST; however, the lack of high temperatures involved in the process makes this explanation unlikely. In any event, the T_C measured for the BST x=0.45 composition (-9 °C) agrees with that measured previously by [1].

The tetragonal ferroelectric to orthorhombic ferroelectric phase transition was observed upon cooling at - 49 °C for the RTF composite produced with BST x=0.3 particles and the conventionally sintered BST x=0.3 pellet. Jin et al. observed [16] this transition at - 40 °C in conventionally sintered BST x=0.3 samples, but rather than conducting their tests upon cooling, they recorded their measurements upon heating, which is generally known to produce less reliable measurements. This difference may have had an impact on the accuracy of their measurements as they also recorded a $T_{\rm C}$ (36 °C) that was 8 °C higher than the $T_{\rm C}$ (28 °C) measured for the conventional BST x=0.3 pellet reported in this work.

Table 5 shows the techniques that were used to improve the density

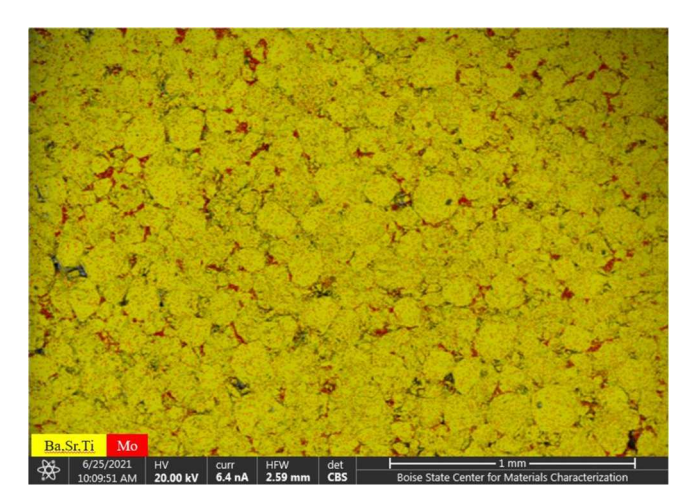


Fig. 5. EDS map of a Ba_{0.5}Sr_{0.5}TiO₃ – LiMoO₄ composite (95.5% dense).

of PZT-LMO RTF composites. In particular, as the volume ratio of Li₂MoO₄ is changed, the density was observed to steadily increase from the 10 vol% composite up to the 17 vol% composite, after which the density was observed to decrease. Thus, 17 vol% Li₂MoO₄ appears to be the ideal amount of binder material to use for the PbZr_yTi_{1-y}O₃ composites, which agrees with recently published work on PZT RTF composites by Nelo et al. [2].

Another factor that was analyzed in this study was mixing different ratios of smaller particles (diameter $<180~\mu m)$ and larger particles (180 $\mu m \leq$ diameter $\leq500~\mu m).$ The ratio that produced the densest composite was an equal mix of larger and smaller particles based on mass. Since the material in both the large particles and small particles is exactly the same, the mass ratio of large to small particles is identical to the volume ratio. According to conventional packing models for bimodal mixtures of non-spherical particles, such as the Furnas model, the ideal ratio should be near 60 vol% larger particles and 40 vol% smaller particles;[17] thus, it is not unreasonable to assume that an equal mix of larger and smaller particles could produce the densest composites based upon the degree to which the particles are misshapen.

For all the composites listed in Table 5, except for those starred, the highest density achievable using particles prepared in this manner was 94.9%; however, once the coating procedure was modified, the density of the final composites was improved to > 95%. This result suggests that the binder material must be dissolved in enough liquid to sufficiently coat all the particles. If more binder material is needed to coat the particles, then it must be dissolved in more liquid and vice versa. It should also be noted that 1.58 g of Li₂MoO₄ can be dissolved in 2 ml of water at 20 °C[3]. So, the amounts of Li₂MoO₄ used in the coating procedure are well within the solubility limit in water.

Energy dispersive X-ray spectroscopy mapping was performed on a cross-section of a PbZr $_{0.5}$ Ti $_{0.5}$ O $_3$ – Li $_2$ MoO $_4$ composite pellet that was 93.4% dense as measured via its outer dimensions and mass. The results of the mapping (Fig. 8) show that Li $_2$ MoO $_4$ is relatively evenly distributed between the PbZr $_{0.5}$ Ti $_{0.5}$ O $_3$ particles as designed. The molybdenum cannot be seen as clearly in this pattern as in Fig. 5 due to the fact that the Pb M $_4$ characteristic X-rays overlap with the Mo L $_4$ ones. It is impossible to deconvolute the spectrum from these two elements; however, the Pb L $_4$ line can be used to determine where Pb does *not* exist within the image, which is within the grain boundary areas. Mo-rich areas also appear as slightly brighter red within the grain-boundary areas. Thus, it is possible to conclude that Li $_2$ MoO $_4$ exists purely in the grain-boundary areas and is relatively evenly distributed throughout the grain boundaries in a manner similar to that observed for the BST-LMO pellet in Fig. 5.

Fig. 9 shows the permittivity of PbZr $_{0.5}$ Ti $_{0.5}$ O $_3$ – Li $_2$ MoO $_4$ and a PbZr $_{0.52}$ Ti $_{0.48}$ O $_3$ – Li $_2$ MoO $_4$ composites as functions of temperature. The composite with PZT y=0.5 particles contained 17 vol% Li $_2$ MoO $_4$ and measured 95.1% dense according to its outer dimensions and mass. The composite with PZT y=0.52 particles also contained 17 vol% Li $_2$ MoO $_4$ and measured 93.9% dense according to its outer dimensions and mass. Since T $_C$ for each of these compositions is well beyond 150 °C, the permittivity should appear as a gradually increasing curve with increasing temperature, as is observed. The room-temperature permittivities were 136.9 and 153.1 for the composites with y=0.5 and y=0.52 particles, respectively, as noted in Table 6.

Table 6 shows that the RTF composites produced in this work retained about 27% of the permittivity value of conventionally sintered analogues. By contrast, the values obtained by Nelo et al.[2] for the RTF pellets made from commercial PZ29 retained just 10% of the value obtained from conventionally sintered PZ29.

4. Conclusions

This work demonstrates that the relative density of roomtemperature fabricated composites can be improved to above 95% reliably and repeatably using the novel technique developed herein. In

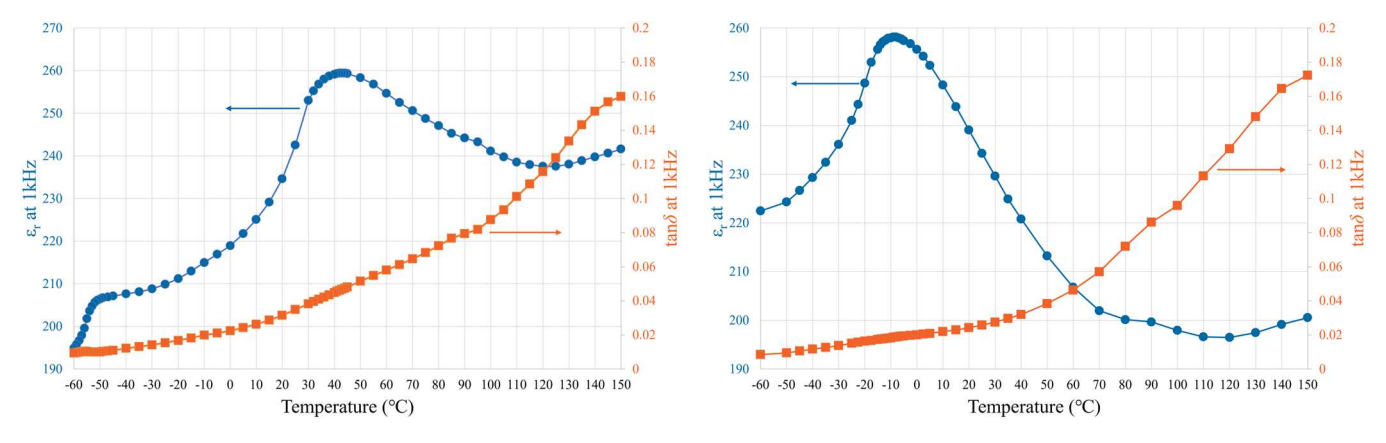


Fig. 6. Permittivity and dielectric loss as functions of temperature for Ba_{0.7}Sr_{0.3}TiO₃ - LiMoO₄ (left) and Ba_{0.55}Sr_{0.45}TiO₃ - LiMoO₄ (right) RTF composites.

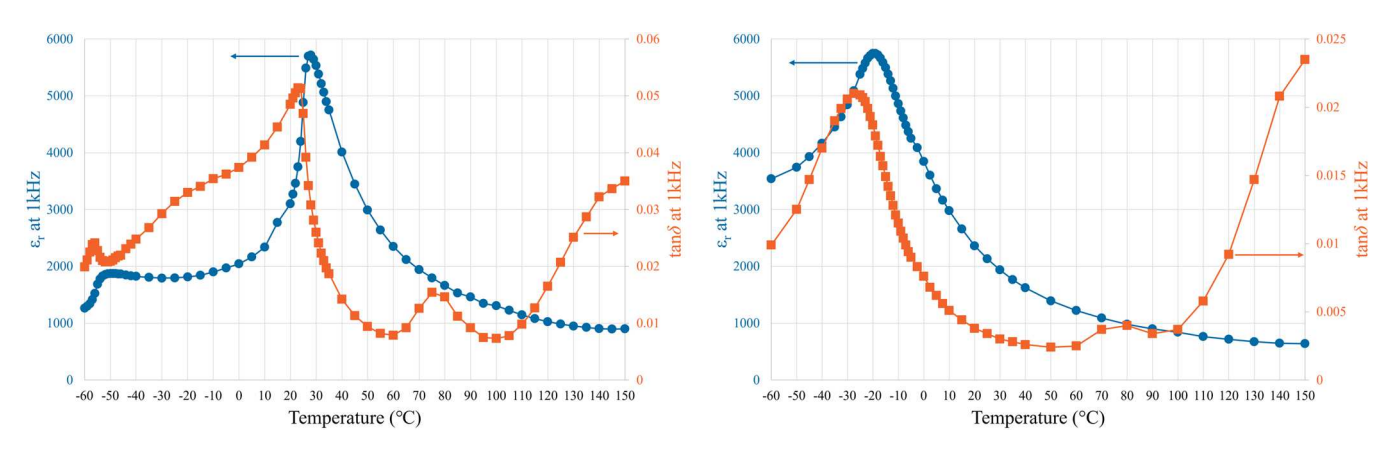


Fig. 7. Permittivity and dielectric loss as functions of temperature for Ba_{0.7}Sr_{0.3}TiO₃ (left) and Ba_{0.55}Sr_{0.45}TiO₃ (right) pellets sintered at 1350 °C for 4 h.

Table 4Dielectric properties of RTF and conventional BST pellets.

Compound	T _C (°C)	$\varepsilon_{\rm r}$ at RT (1 kHz)	tanδ at RT (1 kHz)	Processing Temperature (°C)
BST $x = 0.3$	28	3038	0.0449	1350
BST $x = 0.3$ -	42	235	0.0315	20
BST $x = 0.45$	-20	2365	0.0038	1350
BST $x = 0.45$ - LMO	-9	239	0.0242	20

particular, the most effective strategy to increase the density of these composites involves pressing at high pressure (650 MPa) under a vacuum (60 Torr) then sonicating for 1 min in a bath sonicator before repressing up to 10 times. Ceramics produced in this way contained less than 4% porosity, making them the densest electroceramic composites ever produced using a room-temperature fabrication technique. An EDS map performed on the microstructure of a BST-LMO RTF composite clearly shows that the Li₂MoO₄ binder material is evenly distributed between the BST electroceramic material. Additionally, the dielectric properties of all RTF composites were measured from - 60–150 $^{\circ}\text{C}.$ The permittivities of the composites produced with BST particles are the highest ever recorded for a room-temperature fabricated composite of BST. The T_C values for these RTF composites are also shifted about 11-15 °C higher than those of conventionally sintered pellets with the same composition. Additionally, the permittivities measured for the PZT-LMO composites all showed significant improvements over previous work as compared to conventionally sintered compounds with the same compositions.

The ideal ratio of smaller particles to larger particles was analyzed to

Table 5 Density improvement of $PbZr_yTi_{1\cdot y}O_3 - Li_2MoO_4$ composite RTF pellets using different techniques. All composites were pressed at 650 MPa using a vacuum of 60 torr 10 times. All densities were determined via the dimensions and mass of the pellets.

PZT Compound	vol% LMO	$\begin{array}{l} 0 < PS \\ < 180 \ \mu m \end{array}$	$180~\mu m < PS \\ < 500~\mu m$	Density (%)
y = 0.5	10	_	_	89.5
y = 0.6	10	_	_	90.2
y = 0.6	12	_	_	90.7
y = 0.5	15	_	_	85.1
y = 0.5	16	_	_	92.0
y = 0.5	17	_	_	94.9
y = 0.6	17	-	-	88.2
y = 0.52	17	-	-	91.0
y = 0.5	18	_	_	92.0
y = 0.5	19	_	_	89.3
y = 0.5	17	95 wt%	5 wt%	89.7
y = 0.5	17	90 wt%	10 wt%	91.8
y = 0.5	17	80 wt%	20 wt%	91.5
y = 0.5	17	70 wt%	30 wt%	90.5
y = 0.5	17	60 wt%	40 wt%	91.7
y = 0.5	17	50 wt%	50 wt%	93.4
y = 0.5	17	40 wt%	60 wt%	91.1
y = 0.52	17	40 wt%	60 wt%	88.5
y = 0.5	17	35 wt%	65 wt%	91.5
y = 0.5	17	30 wt%	70 wt%	89.9
y = 0.5	17	10 wt%	90 wt%	89.6
y = 0.52	17	10 wt%	90 wt%	93.7
y = 0.5	17	_	_	95.2a
y = 0.5	17	_	_	95.1a
y = 0.52	17	_	_	93.9a

 $^{^{\}rm a}$ LMO was dissolved in 10 ml of deionized water before 10 ml 1,2-butanediol and PZT particles were added.

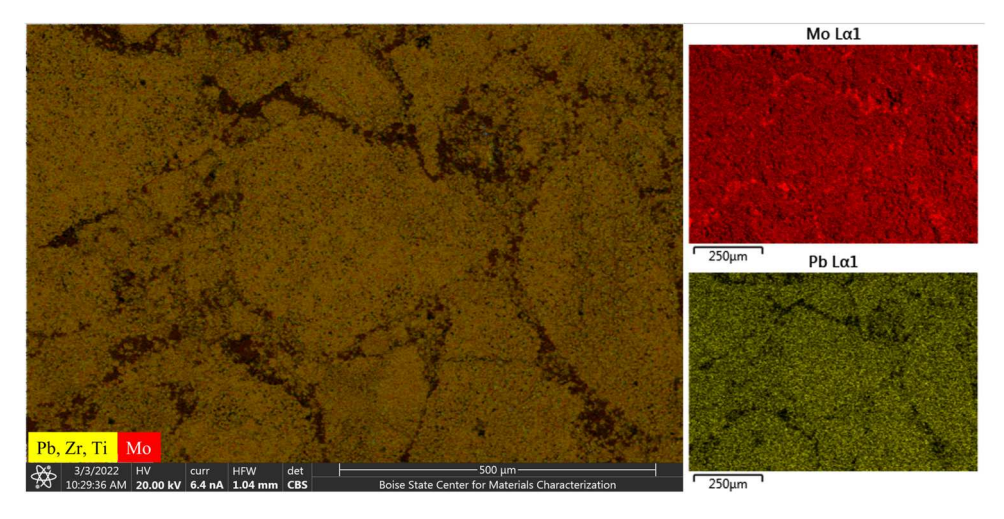
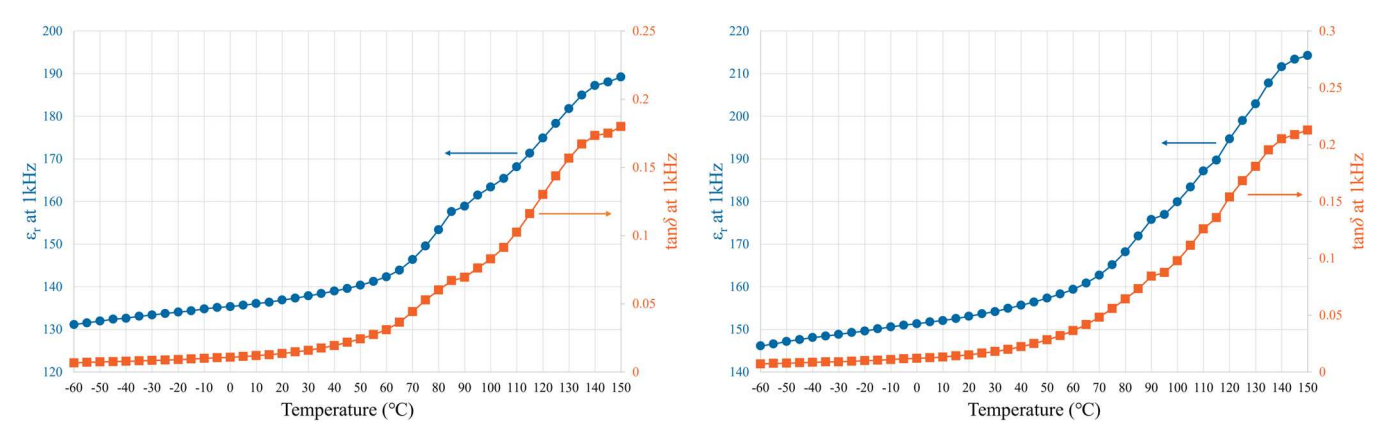


Fig. 8. EDS map of a PbZr_{0.5}Ti_{0.5}O₃-Li₂MoO₄ composite (93.4% dense).



 $\textbf{Fig. 9.} \ \ \text{Permittivity of PbZr}_{0.5}\text{C}_{10.5}\text{O}_{3} - \text{Li}_{2}\text{MoO}_{4} \ (\text{left}) \ \text{and PbZr}_{0.52}\text{Ti}_{0.48}\text{O}_{3} - \text{Li}_{2}\text{MoO}_{4} \ (\text{right}) \ \text{composites as functions of temperature.}$

Table 6Dielectric properties of RTF and conventional PZT pellets.

Compound	T _C (°C)	$\varepsilon_{\rm r}$ at RT (1 kHz)	$tan\delta$ at RT (1 kHz)	Processing Temperature (°C)
PZT $y = 0.5^a$	380	515	0.0050	1200
PZ29 ^b	235	2820	0.0190	1280
PZ29 - LMO ^c		290	0.0510	22
PZT y = 0.5 -		137	0.0135	20
LMO				
PZT y = 0.52 -		153	0.0151	20
LMO				

^a [18]

a degree within the PZT – LMO composite system, and it was determined that the ideal ratio of particles sieved under 180 μ m to particles between 180 μ m and 500 μ m was an equal mass percentage of each.

Declaration of Competing Interest

The authors declare that they have no known competing financial interests or personal relationships that could have appeared to influence the work reported in this paper.

Data availability

The raw data required to reproduce these findings are available to

download from https://data.mendeley.com/datasets/9fp6ps7dsr/1. The processed data required to reproduce these findings are available to download from https://data.mendeley.com/datasets/9fp6ps7dsr/1.

Acknowledgements

This work was supported by the NSF (EAGER grant no. 2040102) and the Micron School of Materials Science and Engineering at Boise State University.

References

- [1] M. Nelo, J. Perantie, T. Siponkoski, J. Juuti, H. Jantunen, Upside-down composites: electroceramics without sintering, Appl. Mater. Today 15 (2019) 83–86.
- [2] M. Nelo, T. Siponkoski, H. Kahari, K. Kordas, J. Juuti, H. Jantunen, Upside-down composites: fabricating piezoceramics at room temperature, J. Eur. Ceram. Soc. 39 (2019) 3301–3306.
- [3] N. Kuzmić, S. Škapin, M. Nelo, H. Jantunen, M. Spreitzer, Dielectric properties of upside-down SrTiO₃/Li₂MoO₄ composites fabricated at room temperature, Front Mater. 8 (2021), 669421.
- [4] F. Bouville, A. Studart, Geologically-inspired strong bulk ceramics made with water at room temperature, Nat. Commun. 8 (2017) 14655.
- [5] J. Guo, H. Guo, A. Baker, M. Lanagan, E. Kupp, G. Messing, C. Randall, Cold sintering: a paradigm shift for processing and integration of ceramics, Angew. Chem. Int. Ed. Engl. 55 (2016) 11457–11461.
- [6] J. Guo, A.L. Baker, H. Guo, M. Lanagan, C.A. Randall, Cold sintering process: a new era for ceramic packaging and microwave device development, J. Am. Ceram. Soc. 100 (2) (2017) 669–677.
- [7] H. Guo, J. Guo, A.L. Baker, C.A. Randall, Cold sintering process for ZrO₂-based ceramics: significantly enhanced densification evolution in yttria-doped ZrO₂, J. Am. Ceram. Soc. 100 (2016) 491–495.

^b [19]
^c [2]

- [8] S. Funahashi, J. Guo, H. Guo, K. Wang, A. Baker, K. Shiratsuyu, C.A. Randall, Demonstration of the cold sintering process study for the densification and grain growth of ZnO ceramics, J. Am. Ceram. Soc. 100 (2) (2016) 546–553.
- [9] H. Guo, J. Guo, A. Baker, C.A. Randall, Hydrothermal-assisted cold sintering process: a new guidance for low-temperature ceramic sintering, ACS Appl. Mater. Interfaces 8 (2016) 20909–20915.
- [10] K. Tsuji, A. Ndayishimiye, S. Lowum, R. Floyd, K. Wang, M. Wetherington, J. P. Maria, C.A. Randal, Single step densification of high permittivity BaTiO₃ ceramics at 300°C, J. Eur. Ceram. Soc. 40 (4) (2020) 1280–1284.
- [11] D. Wang, H. Guo, C. Morandi, C. Randall, S. Trolier-McKinstry, Cold sintering and electrical characterization of lead zirconate titanate piezoelectric ceramics, APL Mater. 6 (2018), 016101.
- [12] B.H. Toby, R.B. Von Dreele, GSAS-II: the gensis of a modern open-source all purpose crystallography software package, J. Appl. Crystallogr. 46 (2) (2013) 544-549
- [13] A. Ianculescu, D. Berger, M. Viviani, C.E. Ciomaga, L. Mitoseriu, E. Vasile, N. Drăgan, D. Crişan, Investigation of Ba_{1-x}Sr_xTiO₃ ceramics prepared from

- powders synthesized by the modified Pechini route, J. Eur. Ceram. Soc. 27 (2007) 3655-3658.
- [14] H. Yokota, N. Zhang, A.E. Taylor, P.A. Thomas, A.M. Glazer, Crystal structure of the rhombohedral phase of Pb(Zr_xTi_{1-x})O₃ ceramics at room temperature. Phys Rev B, Cond. Matter 80 (10) (2009), 104109.
- [15] J. Frantti, J. Lappalainen, S. Eriksson, V. Lantto, S. Nishio, M. Kakihana, et al., Neutron diffraction studies of Pb(Zr_xTi_{1-x})O₃ ceramics, Jpn. J. Appl. Phys. 39 (2000) 5697.
- [16] L. Jin, W. Luo, L. Hou, Y. Tian, Q. Hu, et al., High electric field-induced strain with ultra-low hysteresis and giant electrostrictive coefficient in barium strontium titanate lead-free ferroelectric, J. Eur. Ceram. Soc. 39 (2019) 295–304.
- [17] J. Zheng, W. Carlson, J. Reed, The packing density of binary powder mixtures, J. Eur. Ceram. Soc. 15 (1995) 479–483.
- [18] M. Kumari, A. Singh, J. Mandal, Structural and dielectric properties of PZT ceramics prepared by solid-state reaction route, Int J. Sci. Eng. Res 5 (4) (2014) 404–406.
- [19] Meggit Ferroperm, Ferroperm Matdata 2017, detailed material specifications of Ferroperm piezoceramics, (Meggit A/S, Denmark, 2017).